Journal of Science: Advanced Materials and Devices 5 (2020) 497–501

Contents lists available at ScienceDirect

Journal of Science: Advanced Materials and Devices

journal homepage: www.elsevier.com/locate/jsamd

Original Article

Solution-processable zinc oxide based thin films with different aluminum doping concentrations

Bui Nguyen Quoc Trinh [a, b, *], Truong Dinh Chien [c], Nguyen Quang Hoa [c], Do Hong Minh [d]

[a] Vietnam National University, Hanoi, VNU Vietnam-Japan University, Nanotechnology Program, Luu Huu Phuoc, Nam Tu Liem, Hanoi, Viet Nam
[b] Vietnam National University, Hanoi, VNU University of Engineering and Technology, Key Laboratory for Micro-Nano Technology, 144 Xuan Thuy, Cau Giay, Hanoi, Viet Nam
[c] Vietnam National University, Hanoi, VNU University of Science, Faculty of Physics, 334 Nguyen Trai, Thanh Xuan, Hanoi, Viet Nam
[d] Le Quy Don Technical University, Faculty of Physical and Chemical Engineering, Building S1, 236 Hoang Quoc Viet, Cau Giay, Hanoi, Viet Nam

ARTICLE INFO

Article history:
Received 31 January 2020
Received in revised form
10 August 2020
Accepted 20 August 2020
Available online 27 August 2020

Keywords:
ZnO
AZO
n-type semiconductor
Solar cell
Solution process

ABSTRACT

Al doped zinc oxide (AZO) thin films are attempted to be formed on glass substrates via solution processing with 0, 0.5, 1, 2, 3, and 4 at% Al doping concentrations. Analysis of X-ray diffraction patterns and scanning electron microscopy micrographs indicate that the AZO thin films belong to the wurtzite hexagonal structure with (100), (002), (101), (102), (110), (103), (112) and (201) orientations, and show that the grain size of AZO thin films decreases with higher Al doping concentrations. Optical and electrical properties of the AZO thin films are characterized from using a UV/vis spectrometer and a four-probe measurement system, respectively. The AZO thin films obtained have a minimum sheet resistance of 30.41 Ω/sq for the dopant concentration of 1 at%, and a bandgap energy varying from 3.26 eV to 3.16 eV as the Al doping concentration increases from 0 to 4 at%. The maximum figure of merit value of 7.48×10^{-3} $(\Omega/sq)^{-1}$ corresponds to the deposition of the AZO thin film with 2 at% Al doping.

1. Introduction

In the past decade, transparent conducting oxide (TCO) thin films have gained much attentions for application in electronic devices, including sensors, solar cells, organic light-emitting diodes and flat panel display due to their excellent properties such as high mobility, low resistivity, high transmittance in visible region, high transparency in infrared region [1–4]. Hitherto, the indium tin oxide (ITO) is one of the most commonly-used TCO materials in electronic devices owing to its low resistivity ($\leq 10^{-3}$ Ω cm), low processing temperature (~250 °C) and high optical transparency (> 80%) in the visible region [5]. However, the ITO material has several drawbacks owing to the scarcity, toxicity and high production costs of indium [6], i.e., it is necessary to develop indium-free materials for replacing ITO. Among various indium-free materials, Al-doped zinc oxide (AZO) has been world-wide known as one of the most promising materials for replacing ITO in electronic devices because of its abundance, non-toxicity, high conductivity, high transparency in the visible region and low costs [7,8]. Up to the present time, AZO thin films have been fabricated by various techniques, including chemical vapor deposition [9–11], solution processing [12–14], atomic layer deposition [15–17], pulsed laser deposition [18] and magnetron sputtering [8,19]. Among these methods, the solution-processing method is simplest. It offers distinctive advantages for thin film fabrication because of its low-power and low-material consumption, its possibility of mixing compositions at the molecular level, and its ease to make uniform films over large areas with precise stoichiometry.

Conventionally, most of the AZO thin films prepared by a solution process were deposited on silicon substrates and high-quality Corning glasses, with a relatively high crystalline temperature up to 600 °C. The use of silicon or high-quality glass and the need of high temperatures cause the fabricated products to have high costs if commercialized. Therefore, we limited the annealing temperature in this work to temperatures below 550 °C, and utilized common Deckglasser cover glasses with the purpose of lowering the fabrication costs. Furthermore, we salvaged monoethanolamine (MEA) to stabilize and chelated with zinc acetate via Zn–O bonds at 75 °C. The concentration of Zn^{2+} in solution was kept at 0.5 M. The atomic

* Corresponding author. Vietnam National University, Hanoi, VNU Vietnam-Japan University, Nanotechnology Program, Luu Huu Phuoc, Nam Tu Liem, Hanoi, Viet Nam.
E-mail address: trinhbnq@vnu.edu.vn (B.N.Q. Trinh).
Peer review under responsibility of Vietnam National University, Hanoi.

https://doi.org/10.1016/j.jsamd.2020.08.006

percentage concentration of Al in the precursor solution was varied from 0 to 4 at%. The designed AZO solution was then spin-coated on glass substrates. The annealing temperature was controlled to be 550 °C to match the objective of low-cost substrates in use. The structural, morphological, optical, and electrical properties of the AZO thin films were investigated for film-quality optimization.

2. Experimental

2.1. Precursors formation

A pure ZnO precursor solution was prepared by using zinc acetate dihydrate [$Zn(NO_3)_2 \cdot 2H_2O$] and MEA as a raw material and stabilizer. It was first dissolved in an ethanol solvent of 99% purity, assisted with magnets stirring at room temperature for 15 min to obtain a precursor solution with 0.5 M concentration. Herein, the molecule ratio between [$Zn(NO_3)_2 \cdot 2H_2O$] and MEA was kept at 1:2 for optimum conditions. Second, in order to prepare the AZO precursor solution, different atomic percentage concentrations of Al (0.5, 1, 2, 3 and 4 at%) were added by dissolving the required amount of aluminum nitrate nonahydrate [$Al(NO_3)_3 \cdot 9H_2O$] in the ZnO background solution. Third, the precursor solution was heated at the temperature of 75 °C for 90 min to ensure a complete reaction. Finally, a relevant amount of pure ethanol was added to the precursor solution that was stirred at room temperature for 15 min to regain its initial volume, that is, to resume it to the 0.5 M concentration.

2.2. Thin films preparation

Prior to coating AZO precursor solutions on the surface, the glass substrates were, in turn, cleaned in acetone, ethanol and DI water beakers in an ultrasonic bath for 5 min to remove organic contaminations. Next, the glass substrates were treated in 0.5% HF solution for 30 s to improve hydrophilic ability on the sample surface and to clean metal dusts as well. Thereafter, the AZO precursor solution was dropped on the substrates surface, and spin-coated at a speed of 1500 rpm for 40 s. The samples were then dried at 90 °C for 3 min for each layer. In order to fabricate a desirable thickness, the spin-coating and drying steps were repeated correspondingly. At last, the samples were annealed at a temperature of 550 °C in air for 30 min to obtain crystalline films.

2.3. Characterizations

The crystalline phases of the AZO thin films were identified using an X-ray diffractometer (Bruker D5005, Siemens) at room temperature, with Cu-Kα ($\lambda = 0.154056$ nm) radiation. The surface morphology of the AZO thin films was observed via scanning electron microscopy (Nova NANOSEM-450, FEI), with an operating voltage of 5 kV. The optical transmittance of the AZO thin films was determined using UV/vis spectrophotometer (UV 2450-PC, Shimadzu), and the electrical properties were evaluated by using a four-probe measurement method.

3. Results and discussion

X-ray diffraction (XRD) patterns of the AZO thin films prepared with different Al doping concentrations are plotted in Fig. 1. Diffraction peaks are observed at $2\theta = 31.81°$, 34.51°, 36.34°, 47.62°, 56.68°, 63.04°, 68.20° and 69.22°, and these are well-matched with the standard (100), (002), (101), (102), (110), (103), (112) and (201) orientations corresponding to the wurtzite hexagonal crystal structure of polycrystalline nature (JCPDS 36-1451). No aluminum and other alumina phases were found in the XRD patterns, confirming that the Al ions were successfully substituted into Zn^{2+} ion sites in the ZnO crystal lattice cells. In addition, the peaks of the AZO thin films are well-matched with those of the pure ZnO thin film, suggesting that the Al atoms are incorporated in the ZnO background without any new stress from the difference in the ionic radii of Zn^{2+} and Al^{3+}. The crystallite size of the AZO thin films was calculated from the (101) diffraction peak by using the Debye–Scherrer formula [20].

$$D = \frac{0.9\lambda}{\beta \cos \theta} \quad (1)$$

here, λ and β are the X-ray wavelength and the full width at half maximum (FWHM) of the peak at the Bragg angle, θ, respectively. Consequently, the crystallite size of the AZO thin films decreases from 28.973 nm to 8.612 nm, and the FWHM decreases with increasing Al atomic percentage concentration from 0 to 4 at%, as shown in Table 1. When the Al^{3+} ions substitute into the Zn^{2+} ion sites in the lattice, the proportion of Zn in the AZO thin films decreases, resulting in a decrease in the diffusivity of ZnO by which the growth of grains is retarded [21]. Besides, Al ions can give a

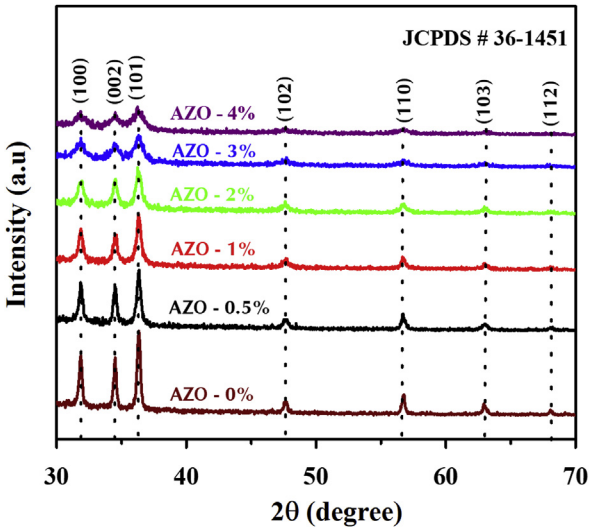

Fig. 1. XRD patterns of AZO thin films with Al doping concentrations varying from 0 to 4 at%.

Table 1
The FWHM value, crystalline size (D), lattice parameters (a, c), stress (ε), dislocation density (δ) calculated for (hkl) = (101) and $2\theta = 36.34°$, and the sheet resistance.

%Al doping	FWHM (°)	D (nm)	a (Å)	c (Å)	ε	δ (10^{-3} nm)	Sheet resistivity (Ω/sq)
0	0.29	28.973	3.2430	5.1944	5.2512	1.1912	70.32
0.5	0.36	23.575	3.2430	5.1944	5.2512	1.7992	38.96
1	0.39	21.288	3.2430	5.1944	5.2512	2.2066	30.41
2	0.51	16.365	3.2430	5.1944	5.2512	3.7339	41.34
3	0.70	12.031	3.2430	5.1944	5.2512	6.9086	129.76
4	0.97	8.612	3.2430	5.1944	5.2512	13.4829	202.13

retarding force at the grain boundary, which can impede the growth of ZnO, that is, can decrease the crystalline size [22].

The lattice strain (ε) and dislocation density (δ) of the AZO thin films were estimated by using the following equations [23].

$$\varepsilon = \frac{\beta}{4\tan\theta} \tag{2}$$

$$\delta = \frac{1}{D^2} \tag{3}$$

The calculated values of ε and δ are indicated in Table 1. The dislocation density of the AZO thin films increases with increasing Al doping concentration from 0 to 4 at%, implying that the quality of the AZO thin films becomes more improved at higher doping concentrations. Furthermore, the crystal lattice parameters (a and c) and the unit-cell volume of the AZO thin films were determined from the preferable diffraction peak (101). As a result, the lattice constants of the AZO thin films are presented in Table 1. No difference in crystal lattice parameters between the different AZO thin films was found. It means that the incorporation of Al^{3+} into Zn^{2+} sites in the ZnO background lattice does not cause any new stress from the difference in the ionic radii of Zn^{2+} and Al^{3+} ($r_{Zn^{2+}} = 0.074$ nm and $r_{Al^{3+}} = 0.054$ nm). The lattice parameters, $a = 3.2430$ Å and $c = 5.1944$ Å, are consistent with the data from standard patterns (JCPDS. 36-1451).

The surface morphology of the AZO thin films with different Al doping concentrations is shown in Fig. 2. It can be seen that the AZO thin film becomes less porous with the increase in Al doping concentration. In addition, the grain size of the AZO thin films decreases with increasing Al doping concentration from 0 to 4 at%. One must note in this work that because the AZO thin films were prepared on glass substrates, it is not precisely correct to evaluate the Al doping level into the ZnO base by using the analysis of the energy dispersive X-ray spectrum. Therefore, a series of AZO thin films should be prepared on Si substrates to have an accurate measurement in a further study.

A four-probe measurement system at room temperature was used to investigate the electrical resistivity for the AZO thin films with different Al doping from 0 to 4 at% as shown in Table 1. For the pure ZnO thin film, the sheet resistance was 70.32 Ω/sq. However, it decreased to 30.41 Ω/sq for the AZO thin film with 1 at% of Al doping. This is due to one additional free electron generated as the Al^{3+} ions substitute the Zn^{2+} ion sites. The sheet resistance slightly increases to 202.13 Ω/sq for the AZO thin film with 4 at% of Al doping. The increase in the sheet resistance might come from the decrease in grain size. As the grain size decreases, a large number of grain boundaries will be generated, leading to a raise in electron collisions and transport time. Also, the excess of Al atoms in the crystal lattice can form some crystal defects (resulting from the difference in the ionic radii of Zn^{2+} and Al^{3+}), leading to the formation of an Al particle cluster nanostructure, which reduces the carrier density and increases the phonon scattering and thus, the sheet resistance increases [24]. The AZO thin film with 1 at% Al doping showed the lowest sheet resistance among the AZO thin films examined which is lower than that reported from other work [25].

The optical transmittance spectra of AZO thin films at different Al doping concentrations were recorded at the wavelength region from 300 to 800 nm, as plotted in Fig. 3. The absorption edge of the AZO thin films was found in the range of 350–400 nm. It has a blue shift with increasing Al doping concentration due to the increase of the bandgap energy. The optical transmission of the AZO thin films increased with increasing Al doping concentration. The transmittance of the AZO thin films is in the range of 68–95%.

Combining the optical and electrical properties to evaluate the suitability of AZO thin films for optoelectronic applications, the figure of merit (ϕ) was calculated by using the following equation [26,27]:

$$\phi = \frac{T^{10}}{R_{sh}} \tag{4}$$

where, T and R_{sh} are the transmittance in visible and near infrared range from 380 to 700 nm and the sheet resistance, respectively.

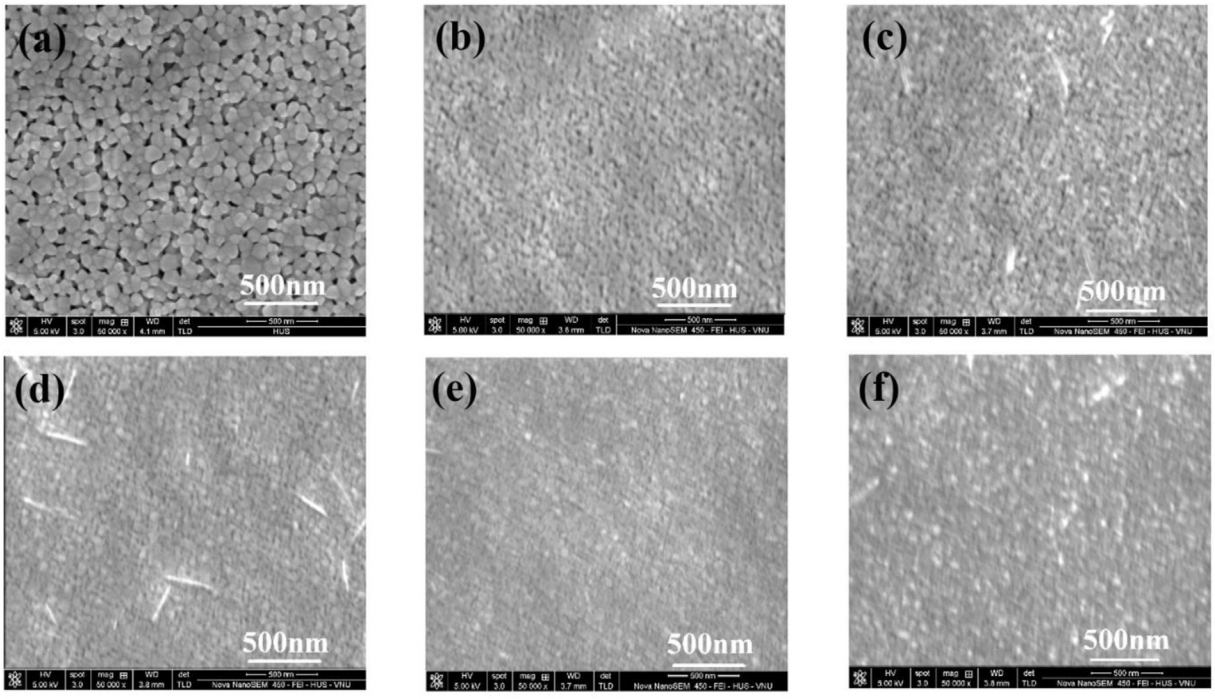

Fig. 2. SEM micrographs of AZO thin films with Al doping concentrations changing from 0 to 4 at%.

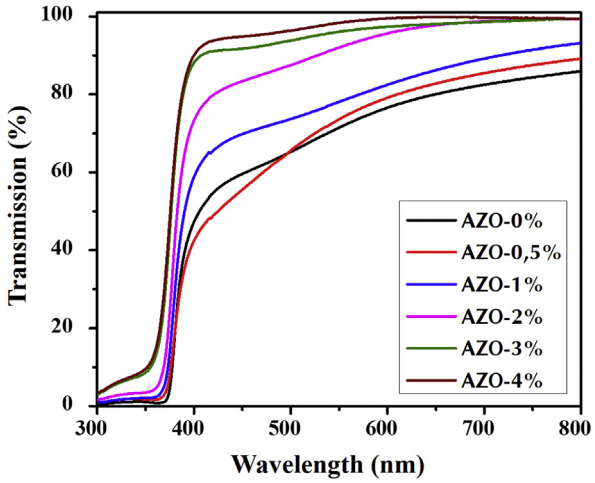

Fig. 3. Transmission spectra of AZO thin films with different Al doping concentrations.

The calculation of ϕ is plotted in Fig. 4, in which the optimum ϕ value of 7.48 $\times$ 10^{-3} $(\Omega/sq)^{-1}$ is obtained for the deposition of an AZO thin film with 2 at% Al doping. This value is comparable, or even higher than the value of 3.05 $\times$ $10^{-3}(\Omega/sq)^{-1}$ reported in previous work by *K. Deva Arun Kumar* et al. [26]. That is, the achieved AZO thin films are suitable for the application of optoelectronic devices.

From Fig. 4, we can also see that the transmittance value of the AZO thin film with 1 at% Al doping is close to that of other common TCO films, which is required for applications in optoelectronic devices [28]. The optical bandgap energy can be determined by using the following equation:

$$\alpha h\upsilon = A\,(h\upsilon\text{-}E_g)^2 \tag{5}$$

here, α is the absorption coefficient, h is Planck's constant, υ is the photon frequency and E_g is the optical-direct bandgap energy [29]. Hence, extrapolation of the linear portion of the $(\alpha h\upsilon)^2$ versus photon energy $(h\upsilon)$ plot as shown in Fig. 5, gives values of E_g, as given in the inset of Fig. 5. From this figure, it is obvious that the optical bandgap of the AZO thin films increases from 3.26 eV for the pure ZnO thin film to 3.31 eV for the AZO thin film with 4 at% Al doping concentration. This trend is consistent with that of other elements doped in ZnO and In_2O_3:Sn films in the TCO materials group [30]. The development of a resonance structure in the density of states, as well as a split of bands owing to the metal dopant act as an ionized donor, resulting in the formation of deep states in the bandgap when the Al doping concentration increases, that is, a blue shift of the bandgap is created as observed [31].

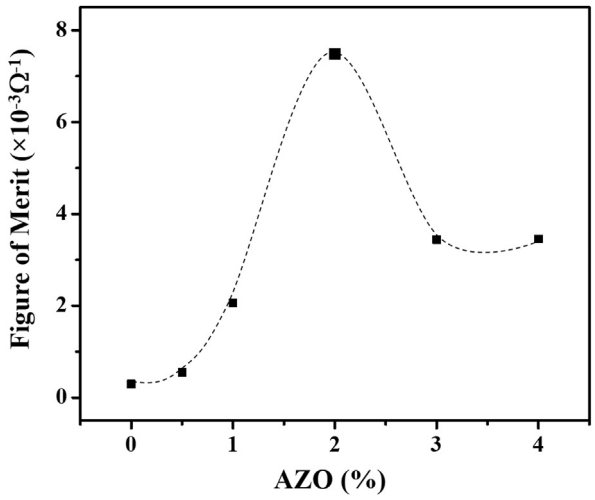

Fig. 4. Figure of merit calculated for the AZO thin films with various Al doping concentrations.

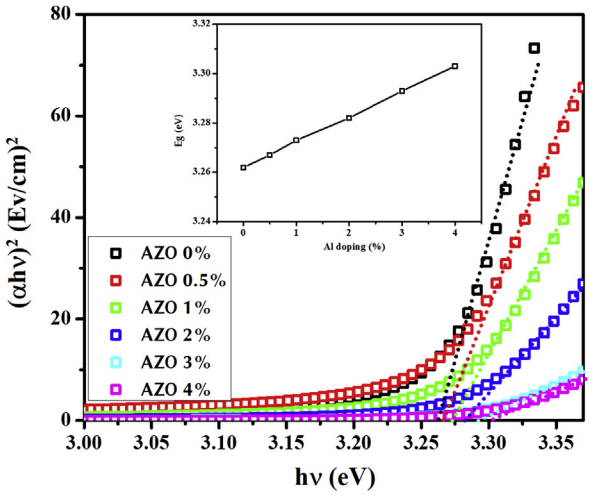

Fig. 5. Tauc plot of AZO thin films. The inset shows the bandgap energy of the AZO thin films.

4. Conclusion

Solution-processed AZO thin films with Al doping concentrations were successfully fabricated on glass substrates. According to XRD results, the AZO thin films are polycrystalline with the wurtzite hexagonal structure, and oriented along (100), (002), (101), (102), (110), (103), (112) and (201) planes. The SEM observation confirmed that the average grain size of the AZO thin films decreases with increasing Al doping concentrations. From transmittance spectra, the bandgap energies of the AZO thin films were determined to be in a range of 3.26–3.31 eV. The minimum sheet resistance of the AZO thin film was found to be 30.41 Ω/sq for 1 at% Al doping. The maximum figure of merit of 7.48 $\times$ 10^{-3} $(\Omega/sq)^{-1}$ is obtained for the AZO thin film with 2 at% Al doping. From different points of view, including low electrical resistivity, high optical transmittance and high figure of merit, the AZO thin films achieved would be applicable in optoelectronic devices.

Declaration of competing interest

The authors declare that they have no known competing financial interests or personal relationships that could have appeared to influence the work reported in this paper.

Acknowledgments

This work was supported by Vietnam National University, Hanoi, under Project No. QG.19.02.

References

[1] M. Berginski, J. Hüpkes, M. Schulte, G. Schöpe, H. Stiebig, B. Rech, M. Wuttig, The effect of front ZnO:Al surface texture and optical transparency on efficient light trapping in silicon thin-film solar cells, J. Appl. Phys. 101 (2007), 074903.

[2] X. Guo, X. Liu, F. Lin, H. Li, Y. Fan, N. Zhang, Highly conductive transparent organic electrodes with multilayer structures for rigid and flexible optoelectronics, Sci. Rep. 5 (2015) 10569.
[3] X. Yu, T.J. Marks, A. Facchetti, Metal oxides for optoelectronic applications, Nat. Mater. 15 (2016) 383.
[4] M.-L. Lin, J.-M. Huang, C.-S. Ku, C.-M. Lin, H.-Y. Lee, J.-Y. Juang, High mobility transparent conductive Al-doped ZnO thin films by atomic layer deposition, J. Alloys Compd. 727 (2017) 565–571.
[5] Y.Y. Kee, S.S. Tan, T.K. Yong, C.H. Nee, S.S. Yap, T.Y. Tou, G. Sáfrán, Z.E. Horváth, J.P. Moscatello, Y.K. Yap, Low-temperature synthesis of indium tin oxide nanowires as the transparent electrodes for organic light emitting devices, Nanotechnology 23 (2011), 025706.
[6] A. Slassi, S. Naji, A. Benyoussef, M. Hamedoun, A. El Kenz, On the transparent conducting oxide Al doped ZnO: first principles and Boltzmann equations study, J. Alloys Compd. 605 (2014) 118–123.
[7] K. Ellmer, Past achievements and future challenges in the development of optically transparent electrodes, Nat. Photonics 6 (2012) 809.
[8] L. Sun, J.T. Grant, J.G. Jones, N.R. Murphy, Tailoring electrical and optical properties of Al-doped ZnO thin films grown at room temperature by reactive magnetron co-sputtering: from band gap to near infrared, Opt. Mater. 84 (2018) 146–157.
[9] S. Saini, P. Mele, T. Oyake, J. Shiomi, J.-P. Niemelä, M. Karppinen, K. Miyazaki, C. Li, T. Kawaharamura, A. Ichinose, Porosity-tuned thermal conductivity in thermoelectric Al-doped ZnO thin films grown by mist-chemical vapor deposition, Thin Solid Films 685 (2019) 180–185.
[10] H.C. Knoops, B.W. van de Loo, S. Smit, M.V. Ponomarev, J.-W. Weber, K. Sharma, W.M. Kessels, M. Creatore, Optical modeling of plasma-deposited ZnO films: electron scattering at different length scales, J. Vac. Sci. Technol. A 33 (2015), 021509.
[11] X.J. Qin, L. Zhao, G.J. Shao, N. Wang, Influence of solvents on deposition mechanism of Al-doped ZnO films synthesized by cold wall aerosol-assisted chemical vapor deposition, Thin Solid Films 542 (2013) 144–149.
[12] M. Shahid, K. Deen, A. Ahmad, M. Akram, M. Aslam, W. Akhtar, Formation of Al-doped ZnO thin films on glass by sol–gel process and characterization, Appl. Nanosci. 6 (2016) 235–241.
[13] M.R. Islam, M. Rahman, S. Farhad, J. Podder, Structural, optical and photocatalysis properties of sol–gel deposited Al-doped ZnO thin films, Surfaces Interfaces 16 (2019) 120–126.
[14] M. Nasiri, S. Rozati, Muscovite mica as a flexible substrate for transparent conductive AZO thin films deposited by spray pyrolysis, Mat. Sci. Semicon. Proc. 81 (2018) 38–43.
[15] Y. Wu, S. Potts, P. Hermkens, H. Knoops, F. Roozeboom, W. Kessels, Enhanced doping efficiency of Al-doped ZnO by atomic layer deposition using dimethylaluminum isopropoxide as an alternative aluminum precursor, Chem. Mater. 25 (2013) 4619–4622.
[16] R.M. Mundle, H.S. Terry, K. Santiago, D. Shaw, M. Bahoura, A.K. Pradhan, K. Dasari, R. Palai, Electrical conductivity and photoresistance of atomic layer deposited Al-doped ZnO films, J. Vac. Sci. Technol. A 31 (2013), 01A146.
[17] C.-H. Zhai, R.-J. Zhang, X. Chen, Y.-X. Zheng, S.-Y. Wang, J. Liu, N. Dai, L.-Y. Chen, Effects of Al doping on the properties of ZnO thin films deposited by atomic layer deposition, Nanoscale Res. Lett. 11 (2016) 407.
[18] H. Zhang, X. Li, Z. Fang, R. Yao, X. Zhang, Y. Deng, X. Lu, H. Tao, H. Ning, J. Peng, Highly conductive and transparent AZO films fabricated by PLD as source/drain electrodes for TFTs, Materials 11 (2018) 2480.
[19] H. Park, S.Q. Hussain, S. Velumani, A.H.T. Le, S. Ahn, S. Kim, J. Yi, Influence of working pressure on the structural, optical and electrical properties of sputter deposited AZO thin films, Mat. Sci. Semicon. Proc. 37 (2015) 29–36.
[20] S. Maniv, A. Zangvil, Controlled texture of reactively rf-sputtered ZnO thin films, J. Appl. Phys. 49 (1978) 2787–2792.
[21] S. Neogi, S. Chattopadhyay, A. Banerjee, S. Bandyopadhyay, A. Sarkar, R. Kumar, Effect of 50 MeV Li^{3+} irradiation on structural and electrical properties of Mn-doped ZnO, J. Phys. Condens. Mat. 23 (2011) 205801.
[22] S. Fujihara, C. Sasaki, T. Kimura, Effects of Li and Mg doping on microstructure and properties of sol-gel ZnO thin films, J. Eur. Ceram. Soc. 21 (2001) 2109–2112.
[23] X. Wang, Z. Wu, J. Webb, Z. Liu, Ferroelectric and dielectric properties of Li-doped ZnO thin films prepared by pulsed laser deposition, Appl. Phys. A 77 (2003) 561–565.
[24] B. Joseph, P. Manoj, V. Vaidyan, Studies on the structural, electrical and optical properties of Al-doped ZnO thin films prepared by chemical spray deposition, Ceram. Int. 32 (2006) 487–493.
[25] G. Wu, Y. Chen, H. Lu, Aluminum-doped zinc oxide thin films prepared by sol-gel and RF magnetron sputtering, Acta Phys. Pol. A 120 (2011) 149–152.
[26] K. Deva Arun Kumar, S. Valanarasu, S. Rex Rosario, Evaluation of the structural, optical and electrical properties of AZO thin films prepared by chemical bath deposition for optoelectronics, Solid State Sci. 78 (2018) 58–68.
[27] G. Haacke, New figure of merit for transparent conductors, J. Appl. Phys. 47 (1976) 4086–4089.
[28] J. Mendez-Gamboa, R. Castro-Rodriguez, I. Perez-Quintana, R. Medina-Esquivel, A. Martel-Arbelo, A figure of merit to evaluate transparent conductor oxides for solar cells using photonic flux density, Thin Solid Films 599 (2016) 14–18.
[29] X. Zhang, K.S. Hui, K. Hui, High photo-responsivity ZnO UV detectors fabricated by RF reactive sputtering, Mater. Res. Bull. 48 (2013) 305–309.
[30] H. Fujiwara, M. Kondo, Effects of carrier concentration on the dielectric function of ZnO: Ga and In_2O_3: Sn studied by spectroscopic ellipsometry: analysis of free-carrier and band-edge absorption, Phys. Rev. B 71 (2005), 075109.
[31] F. Yakuphanoglu, S. Ilican, M. Caglar, Y. Caglar, Microstructure and electro-optical properties of sol–gel derived Cd-doped ZnO films, Superlattice, Microst 47 (2010) 732–743.